Vibrational Dynamics of Polyaniline Pernigraniline Base Form: A Conducting Polymer

Abhishek Kumar Mishra,[*1] *Poonam Tandon,*[2] *V. D. Gupta*[2]

Summary: Polyaniline is unique among conducting polymers in that its electrical properties can be reversibly controlled both by the oxidation state of the main chain and by protonation. In the present communication we report normal modes and their dispersion in polyaniline pernigraniline base (PANI PNB) form using Urey - Bradely force field which in addition to valence force field accounts for the non-bonded interactions in the *gem* and *cis* configurations and tension terms. Some of the distinguished features of the dispersion curves such as cross-over and Von Hove type of singularities are discussed and possible explanations are given in terms of symmetry considerations. Several new assignments, which are missing in earlier work, are reported.

Keywords: cross-over; density-of-states; dispersion curves; pernigraniline base form; polyaniline

Introduction

Since the discovery of metal like electrical conductivity in polyacetylene, there have been various studies on the physical and chemical properties of conjugated electroactive polymers. Among them, members of Polyaniline(PANI) have received considerable attention due to the controllable electrical conductivity[1], environmental stability[2], and interesting redox properties associated with the chain hetroatoms.[3]

Polyaniline, a green intractable powder, has a history beginning more than 120 years ago, when in 1862 Letheby[4] reported on the electrochemical oxidation product of aniline and in 1968 Surville et al.[5] on the high electrical conductivity and its pure electronic character in PANI, which depends on the ''acidity, redox level & hydration''[5] of the polymer. PANI was rediscovered few years ago as a very important member of conducting polymers having wide potential technological applications.[6–11] Polyaniline is also used as an electrode material for semiconductor batteries,[9,12–16] as a semiconducting material,[17] as a sensor material,[18] as an electrochromic-display material[19–21] and as a catalyst for photoelectrochemical processes.[21]

Polyaniline relates to a large class of polymers insofar as several forms of these compounds can be obtained. These different forms are described by two parameters: the average oxidation state[22,23] and the degree of protonation.[24] These conducting polymers differ substantially from polyacetylene and other aromatic and hetroaromatic polymers in the fact that their electronic structure is based on the overlap of alternating nitrogen and C6 rings. In its nonconductive undoped (or base) form, Polyaniline have the general formula $[(–B–NH–B–NH–)_y\ (–B–N=Q=N–)_{1-y}]_x$, (B and Q stands for benzenoid and quinoid structure respectively) where y can be varied continuously from one to zero (from completely reduced form to the completely oxidized one). The conversion to a conductive form can be accompolished by either protonic or electronic doping.[25]

[1] Department of Physics, Amity School of Engineering, Amity Institute of Applied Sciences, Amity University, Noida 201 301, India
E-mail: mishra_lu@hotmail.com
[2] Department of Physics, University of Lucknow, Lucknow-226007, India

The terms leucoemeraldine, emeraldine, and pernigraniline refer to the different oxidation states of the polymer where y = 1, ~0.5, and 0, respectively. In this work we have focussed our all attention on the fully oxidized (y = 0) non protonated form (Pernigraniline Base: PNB).

Since the electronic properties of the compounds are directly associated to the chemical bondings and the electron distribution along the polymer backbone, a clear knowledge of their vibrational properties can be of major importance. Vibrational spectroscopy plays an important role in the elucidation of polymeric structure. Normal mode analysis besides identification of various modes provides an insight into Infrared absorption (IR), Raman spectra and Inelastic Neutron Scattering (INS). An overall understanding of vibrational dynamics in a polymer involves calculation of the dispersion curves. These curves provide knowledge of degree of uninterrupted sequence lengths in an ordered conformation.

This is the first communication in which the complete planar and non-planar normal coordinate analysis of PANI Pernigraniline (PNB) form along with the dispersive behaviour of the normal modes is being reported. We present here a normal mode analysis of PANI PNB form with phonon dispersion in the first Brillouin Zone using Urey Bradley force field (UBFF).[26,27] Earlier works on normal mode analysis[28–30] of Lefrant and co-workers using valence force field suffers from the use of approximate force field resulting in the inaccurate and incomplete assignments specially in the lower region of spectra and lack of dispersion curves. For the full understanding of vibrational spectra, it is necessary to know the dispersive nature of normal modes. Such studies also provide information on the degree of coupling and dependence of the frequency of a given mode on the sequence length of the ordered conformation. These curves are also useful in calculating the density of vibrational states which in turn can be used for obtaining thermodynamic properties such as specific heat, entropy, enthalpy and free energy. Our calculations are based on UBFF, which in addition to valence force field accounts for the non-bonded interactions in the *gem* and *cis* configuration and the tension terms. In this force field the potential energy expression does not have quadratic cross terms. The force constants are supplemented by the repulsive forces between non-bonded atoms, which simulate the Van der Waals force[31] between them. It gives a better description of intra and inter unit interactions, and arbitrariness in choosing the force constants is reduced, thereby enabling us to arrive at a better unique force field.

This paper provides a better understanding of the PANI PNB spectra by assigning bands based on para-disubstituted benzene derivatives. It is often difficult to describe a vibration completely using symbols or descriptions; therefore describing the modes based on substituted benzene modes should give a complete understanding of the vibrational modes of PANI PNB form. Many authors have examined benzene derivatives [32–39] and made assignments that have been used in this work to assign the modes of PANI PNB form. One of the most comprehensive discussions is that of Varsanyi.[32] For purposes of assigning fundamental modes, PANI is considered to be ''di-light'', since N has an atomic weight below 14.

Theory

Calculation of Normal Mode Frequencies

Normal mode calculation for a polymeric chain was carried out using Wilson's GF matrix method[40,41] as modified by Higgs[42] for an infinite polymeric chain. The vibrational secular equation to be solved is?

$$|G(\delta)F(\delta) - \lambda(\delta)I| = 0 \quad 0 \le \delta \le \pi \qquad (1)$$

where δ is the phase difference between the modes of adjacent chemical units, $G(\delta)$ is the inverse kinetic energy matrix and $F(\delta)$ is the force field matrix for a certain phase value. The wavenumber $\bar{\nu}_i(\delta)$ in cm^{-1} are related to eigen values by $\lambda_i(\delta) = 4\pi^2c^2\ [\bar{\nu}_i(\delta)]^2$.

A plot of $\bar{\nu}_i(\delta)$ versus δ gives the dispersion curve for the i[th] mode. The use of the type of force field is generally a matter of one's chemical experience and intuition.[43] In the present work, we have used Urey-Bradley force field as it is more comprehensive then valence force field. The Urey-Bradley takes in to account both bonded and non-bonded interactions as well as internal tensions. Potential energy for this force field can be written as

$$V=\sum_{m,j,k} K'_{j,k} r^{(m)}_{j,k}\left(\Delta r^{(m)}_{j,k}\right)+K_{j,k}\left(\Delta r^{(m)}_{j,k}\right)^2/2+\sum_{m,i,j,k} H'_{i,j,k} r^{(m)}_{i,j} r^{(m)}_{j,k}\left(\Delta\alpha^{(m)}_{i,j,k}\right)+H_{i,j,k} r^{(m)}_{j,k}\left(\Delta\alpha^{(m)}_{i,j,k}\right)^2/2 + \sum_{m,i,j,k} F'_{i,k} q^{(m)}_{i,k}\left(\Delta q^{(m)}_{i,k}\right)+F_{i,k}\left(\Delta q^{(m)}_{i,k}\right)^2/2+\sum_j K^{\tau}_j\left(\Delta\tau_j\right)^2+\sum_j K^{\omega}_j\left(\Delta\omega_j\right)^2 \quad (2)$$

where the symbols have their usual meaning. The primed quantities are introduced as internal tensions. Non-bonded interactions involve attraction and repulsion of atoms due to the overlap of their electron shells. These effects are usually expressed by the 6-exp or 6-12 type potentials. The tension terms are assumed to be all zero.

Recently, spectroscopically effective molecular mechanics model have been used for inter and intra molecular interactions consisting of charges, atomic dipoles and Vander Waals (non bonded) interactions.[31]

The force constants, including those for the interaction of first and third non-bonded atoms, which give the ''best fit'', are given in the Table 1 and have been obtained by least squares fitting. In order to obtain the ''best fit'' with the observed wavenumbers the following procedure is adopted.

Starting with the approximate F matrix F_o and observed frequencies λ_{obs} (related through a constant), one can solve the secular matrix equation:

$$GF_0L_0 = L_0\lambda_0 \quad (3)$$

Let $\Delta\lambda_i = \lambda_{i_{obs}} - \lambda_{i_0}$ in the above equation. It can be shown that in the direct order of approximation

$$\Delta\lambda = J\Delta F \quad (4)$$

where J is computed from L_0. We wish to compute the corrections to F_0 so that the errors $\overline{\Delta\lambda}$ are minimized. We used the theory of least squares and calculate

$$J'P\overline{\Delta\lambda} = (J'PJ)\overline{\Delta F} \quad (5)$$

where P is the weighting matrix and J′ is the transposition of J. The solution of this equation is obtained by inverting J′PJ to give

$$\overline{\Delta F} = (J'PJ)^{-1}J'P\overline{\Delta\lambda} \quad (6)$$

If the number of frequencies is greater than the number of F matrix elements, the matrix J′PJ should be non-singular and we obtain the corrections ΔF, which will minimize the sum of the weighted squares of the residuals. This minimum sum provides the ''best fit''. If the corrections ΔF are fairly large, the linear relation between force constant and frequency term in the matrix Equation (3) breaks down. In such a situation, further refinement using higher order terms in the Taylor's series expansion of $\Delta\lambda_i$ is needed. King et al.[44] developed this procedure.

Table 1.
Internal Coordinates and force Constants for PANI PNB form (md/Å).

Internal coordinates	Force Constants	Internal coordinates	Force Constants
ν[C–C]*	5.05	φ[C–C–C]$	0.38(0.40)
ν[C–H]	4.74	φ[C–C–H]$	0.415(0.46)
ν[C=C]*	5.40	φ[C–C=C]$	0.42(0.35)
ν[C–N]	4.41	φ[H–C=C]$	0.20(0.35)
ν[N=C]	5.40	ω[C–H]	0.27
ν[C–C]$	4.14	ω[C–N]	0.368
ν[C=C]$	5.35	ω[N=C]	0.28
φ[H–C–C]*	0.30(0.30)	τ[C=C]*	0.033
φ[H–C=C]*	0.42(0.39)	τ[C–C]*	0.037
φ[C–C=C]*	0.69(0.50)	τ[C–N]	0.030
φ[C–C–N]	0.43(0.42)	τ[N=C]	0.030
φ[C=C–N]	0.43(0.42)	τ[C–C]$	0.032
φ[C–N=C]	0.425(0.40)	τ[C=C]$	0.042
φ[N=C–C]	0.68(0.58)		

Note: ν, φ, ω and τ denote stretch, angle bend, wag and torsion respectively. Non-bonded force constants are given in parentheses. * and $ corresponds to benzoid and quinoid rings respectively.

Results and Discussion

A chemical repeat unit of PANI PNB consists of one benzoid ring and one quinoid ring (Figure 1). The number of atoms in the repeat unit are 22 which give rise to 3N-4 = 62 normal modes which would be optically active and 4 acoustical modes which correspond to three translations and one rotation about the backbone. Initially Force constants from some similar molecules are transferred and later modified to give the ''best fit'' to the observed infrared and Raman frequencies.[29–30] The vibrational wave numbers were calculated for values of δ varying from 0 to π in steps of $.05\pi$. The assignments have been made on the basis of potential energy distribution (PED), absorption band shape, band intensity and absorption/scattering due to molecular groups placed in similar environments. Final sets of force constants along with the internal coordinate are given in Table 1. The force field (Table 1) thus obtained is also well supported with by the experimental spectra and one can get a very good fit frequencies without changing the off-diagonal elements. The observed Raman and IR[29,30] and calculated frequencies along with their potential energy distribution (PED) at the zone centre and zone boundary are given in Table 2. Since all the modes above 900 cm^{-1} are non-dispersive or have negligible dispersion, the dispersion curves are plotted only for the modes below 900 cm^{-1}. The lowest two branches of the dispersion curves correspond to the four acoustic modes. Out of these, three are due to the translation (one parallel and two perpendicular to the chain axis) and one due to rotation around the chain. Our spectral interpretation is also based on the fundamental p-disubstituted benzene modes and the assignments of the modes are discussed according to their nature of vibrations.

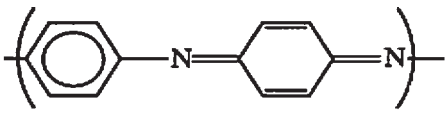

Figure 1.
One chemical repeat unit of Polyaniline PNB form.

C–H Stretching Vibrations

There C–H stretching vibrations of benzene derivatives generally appear above 3000 cm^{-1}. Vibrations 2, 7b, 20a and 20b are C–H stretching vibrations in p-disubstituted benzene derivatives and correspond to phase combinations: + + + +, + − + −, + − − + and + + + + respectively. By our l-vector calculations of PANI PNB form we found that calculated normal modes at 3087, 3086, 3085, 3084 corresponds to 20b, 20a, 2, 7b vibrations of the quinoid ring and 3072, 3069, 3068 and 3065 cm^{-1} corresponds to 20b, 20a, 2, 7b C–H stretching vibrations of the benzoid ring.

C–C Stretching Vibrations

Wilson no. 8a, 8b, 19a, 19b and 14 are associated with CC stretching vibrations. Two well resolved Raman bands at 1612 and 1579 cm^{-1} are assigned to the calculated normal modes at 1623 and 1580 cm^{-1} respectively. These two bands are found to be associated with CC stretching vibrations and can be seen as 8a vibrations of the benzoid and quinoid rings. The characteristic infrared band at about 1570 cm^{-1} is assigned to the quinoid unit (8b) while the 8b vibration of the benzoid ring can be seen as Raman peak at 1555 cm^{-1}.19b Wilson vibration of the quinoid and benzoid rings are calculated at 1415 and 1398 cm^{-1} and are assigned to the bands at 1418 (Raman) and 1411(IR) cm^{-1} respectively. Infrared band at 1495 cm^{-1}[45] can be seen as 19a Wilson C–H stretching vibration and while the band at 1377 cm^{-1} is related with CC stretching + CH bending vibration of the quinoid ring (14).

C–H Bending Vibrations

In p-disubstituted benzenes, normal vibrations 3, 9a, 18b and 18a are classified as modes having C–H in-plane bending character. The vibration 3 appears generally as a weak absorption in the infrared spectra and in the PANI PNB form spectra we have a absorption dip at 1315 cm^{-1} which can be assigned to the modes calculated at 1327,

Table 2.
Calculated and Observed Modes of PANI PNB

Cal. freq.	Obs. Freq.		Assignment (% PED), $\delta = 0$	Cal. freq	Obs. Freq.		Assignment (% PED), $\delta = \pi$
	Raman	IR			Raman	IR	
3087	–	–	ν[C–H]$(99)	3087	–	–	ν[C–H]$(99)
3086	–	–	ν[C–H]$(99)	3086	–	–	ν[C–H]$(99)
3085	–	–	ν[C–H]$(99)	3085	–	–	ν[C–H]$(99)
3084	–	–	ν[C–H]$(99)	3084	–	–	ν[C–H]$(99)
3072	–	–	ν[C–H]*(99)	3072	–	–	ν[C–H]*(99)
3069	–	–	ν[C–H]*(99)	3070	–	–	ν[C–H]*(99)
3068	–	–	ν[C–H]* (99)	3068	–	–	ν[C–H]* (99)
3065	–	–	ν[C–H]* (99)	3065	–	–	ν[C–H]* (99)
1623	1612[a]	–	ν[C=C]*(29) + ν[C–C]*(27) + φ[H–C=C]*(12) + ν[C–N](10) + φ[C–C=C]*(9) + φ [H–C–C]*(9)	1623	1612[a]	–	ν[C=C]* (30) + ν[C–C]* (27) + φ[H–C=C]*(12) + ν[C–N](10) + φ[C– C=C]*(9) + φ[H–C–C]* (9)
1580	1579[a]	1570[a]	ν[C=C]$(33) + ν[C–C]$(20) + φ[C–C–H]$(18) + ν[N=C](13)	1583	1579[a]	1570[a]	ν[C=C]$ (30) + ν[C–C]$ (19) + φ[C–C–H]$(17) + ν[N=C](15)
1562	–	1570[a]	ν[C–C]*(41) + ν[C=C]*(28) + φ[H–C=C]*(14) + φ[C–C=C]*(8) + φ[H–C–C]*(6)	1562	–	1570[a]	ν[C–C]*(40) + ν[C=C]*(29) + φ[H–C=C]*(13) + φ[C–C=C]*(8) + φ[H–C–C]* (6)
1558	1555[a]	–	ν[C=C]*(48) + ν[C–C]*(41) + φ[H–C=C]*(5)	1558	1555[a]	–	ν[C=C]*(48) + ν[C–C]* (41) + φ[H–C=C]*(5)
1545	1555[a]	–	ν[C=C]* (24) + ν[C–N](19) + φ[H–C=C]*(18) + φ[H–C–C]*(15)	1539	1555[a]	–	ν[C=C]* (25) + φ[H–C=C]*(21) + φ[H–C–C]*(18) + ν[C–N](16)
1496		1495[c]	ν[C=C]$(53) + ν[C–C]$(26) + φ[C–C–H]$(18) + φ[H–C=C]$(6)	1496		1495[c]	ν[C=C]$(53) + ν[C–C]$(26) + φ[C–C–H]$(15) + φ[H–C=C]$(6)
1487	1480[a]	1480[a]	ν[N=C](31) + ν[C–C]$(20) + φ[C–C–H]$(20) + φ[H–C=C]$(9)	1493	1480[a]	1480[a]	ν[N=C](38) + ν[C–C]$(21) + φ[C–C–H]$(20) + φ[H–C=C]$(9)
1415	1418[a]	–	ν[C–C]$(76) + φ[N=C–C](10) + φ[C–C=C]$(6) + φ[H–C=C]$(6)	1417	1418[a]	–	ν[C–C]$(71) + φ[N=C–C](10) + φ[C–C=C]$(6) + φ[H–C=C]$(6)
1398	–	1411[a]	φ[H–C=C]*(20) + ν[C=C]*(19) + ν[C–C]*(15) + φ[H–C–C]*(14) + ν[C–C]$(11)	1393	–	1411[a]	φ[H–C=C]*(24) + ν[C=C]* (23) + ν[C–C]*(17) + φ[H–C–C]*(17) + ν[C–C]$(6)
1381	–	1377[a]	ν[C–C]$(41) + φ[C–C–H]$(17) + φ[N=C–C](12) + φ[H–C=C]*(6) + ν[C=C]*(5) + φ[H–C=C]$(5)	1385	–	1377[a]	ν[C–C]$(52) + φ[C–C–H]$(21) + φ[N=C–C](16) + φ[H–C=C]$ (6)
1371	–	1377[a]	ν[N=C](45) + ν[C–N](22) + ν[C=C]$(16)	1367	–	1377[a]	ν[N=C](41) + ν[C–N](17) + ν[C=C]$(15) + φ[H–C=C]*(9) + a[H–C–C]*(6)
1334		–	φ[H–C=C]*(36) + φ[H–C–C]*(18) + ν[C–N](9) + φ[C–C–H]$(8) + φ[H–C=C]$(6) + ν[C=C]*(5) + φ[C–C=C]*(5)	1327		–	φ[H–C=C]*(48) + φ[H–C–C]*(31) + ν[C=C]*(6)
1324		–	φ[C–C–H]$(58) + φ[H–C=C]$(30)	1324	1320[b]	–	φ[C–C–H]$(61) + φ[H–C=C]$(31)
1317		1315[a]	φ[H–C=C]*(21) + φ[H–C–C]*(20) + φ[C–C–H]$(14) + ν[C–N](13) + φ[H–C=C]$(11) + ν[N=C](10)	1323	1320[b]	1315[a]	ν[C–N](27) + φ[C–C–H]$(21) + φ[H–C=C]$(17) + ν[N=C](16) + ν[C–C]*(6)
1217	1215[a]	1211[a]	ν[N=C](23) + ν[C–N](16) + φ[C–C=C]*(14) + φ[H–C=C]$(12) + φ[C–C–H]$(10) + φ[H–C–C]*(8) + φ[H–C=C]*(7)	1219	1215[a]	1211[a]	ν[C–N](23) + ν[N=C](19.72) + φ[C–C=C]*(17) + φ[H–C–C]*(11) + φ[H–C=C]*(10) + ν[C=C]$(7)
1214	1215[a]	1211[a]	ν[C–N](26) + ν[N=C](16) + φ[H–C=C]*(15) + ν[C–C]*(11) + φ[H–C–C]*(10) + [C=C]*(7) + ν[C=C]$(6)	1205	1215[a]	1211[a]	φ[H–C=C]*(17) + ν[C–N](17) + ν[N=C](16) + φ[H–C–C]*(12) + φ[H–C=C]$(8) + ν[C–C]*(8) + φ[C–C–H]$(7)
1176	–	1164[c]	φ[H–C=C]*(32) + ν[C=C]*(26) + φ[H–C–C]*(20) + ν[C–C]*(7) + ν[C–N](7)	1175	–	1164[c]	φ[H–C=C]*(29) + ν[C=C]*(26) + φ[H–C–C]*(18) + ν[C–N](8) + ν[C–C]*(8)
1154	1157[a]	1157[a]	φ[C–C–H]$(45) + φ[H–C=C]$(29) + ν[C=C]$(20)	1154	1157[a]	1157[a]	φ[C–C–H]$(45) + φ[H–C=C]$(29) + ν[C=C]$(19) + ν[C–C]$(5)
1087	–	1098[a]	φ[C–C–H]$(25) + ν[C=C]$(24) + φ[H–C=C]$(22) + ν[C–C]$(11) + φ[N=C–C](11)	1088	–	1098[a]	φ[C–C–H]$(26) + ν[C=C]$(25) + φ[H–C=C]$(23) + φ[N=C–C](12) + ν[C–C]$(11)

(*Continues*)

Table 2.
(Continued)

Cal. freq.	Obs. Freq.		Assignment (% PED), $\delta = 0$	Cal. freq	Obs. Freq.		Assignment (% PED), $\delta = \pi$
	Raman	IR			Raman	IR	
1008	–	1006[a]	φ[C–C=C]*(32) + ν[C–C]*(25) + ν[C=C]*(17) + φ[H–C–C]*(14) + φ[H–C=C]*(12)	1008	–	1006[a]	φ[C–C=C]*(32) + ν[C–C]*(25) + ν[C=C]*(17) + φ[H–C–C]*(14) + φ[H–C=C]*(12)
978	–	965[c]	ω[C–H](78) + ω[C–N](9)	976	–	965[c]	ω[C–H](77) + ω[C–N](11)
966	–	965[c]	ω[C–H](83) + t[C=C]$(7)	969	–	965[c]	ω[C–H](81) + t[C=C]$(8) + ω[N=C](6)
953	–	954[a]	ν[C–C]$(58) + φ[C–C=C]$(20.52) + φ[C–C–H]$(17)	951	–	954[a]	ν[C–C]$(54) + φ[C–C=C]$(21) + φ[C–C–H]$(16)
948	–	954[a]	ω[C–H](82) + t[C=C]$(13)	948	–	954[a]	ω[C–H](82) + t[C=C]$(13)
938	–	931[c]	ω[C–H](83) + t[C–C]*(8) + t[C=C]*(8)	939	–	931[c]	ω[C–H](83) + t[C–C]*(8) + t[C=C]*(8)
866	–	–	ν[C–C]*(30) + ν[C=C]*(25) + ν[C–C]$(17) + ν[C–N](12) + φ[C–C=C]*(7)	861	–	–	ν[C–C]*(30) + ν[C=C]*(26) + ν[C–N](13) + φ[C–C=C]*(8)
842	848[a]	844[a]	ω[C–H](55) + ω[C–N](17) + φ[C–N=C](11) + ω[N=C](6)	841	848[a]	844[a]	ω[C–H](33) + ν[C–C]$(30) + ω[c–N](14) + ν[C=C]$(7)
807	790[b]		ω[C–H](45) + φ[C–C=C]*(8) + ν[C–N](7) + ω[N=C](7) + φ[C–C=C]$(6)	823	–	–	ω[C–H](32) + ν[C–C]$(22) + φ[C–C=C]*(8) + ω[C–N](8) + ν[C–N](7)
790	790[b]	–	ν[C–C]$(47) + ν[N=C](9) + ν[C=C]$(6) + φ[C–C=C]*(6) + φ[C–N=C](5)	802	790[b]	–	ω[C–H](67) + ω[N=C](12) + τ[C–C]$(6) + φ[C–N=C](5)
776		–	ω[C–H](38) + φ[C–C=C]$(10) + ν[C–N](10) + φ[C–C=C]*(9) + φ[C–C–C]$(7) + φ[N=C–C](5)	761		–	ω[C–H](85) + τ[C–C]*(8) + τ[C=C]*(7)
761	–	775[a]	ω[C–H](85) + τ[C–C]*(7) + τ[C=C]*(7)	752	–	775[a]	ω[C–H](86) + τ[C–C]$(14)
752		750[b]	ω[C–H](86) + τ[C–C]$(14)	718	–	–	ν[C–N](20) + ω[C–H](13) + φ[C–N=C](13) + φ[C–C=C]*(12) + ν[C–C]$(10) + ω[N=C](6)
658	–	–	ω[C–H](27) + φ[C–N=C](21) + ν[C–N](9) + ν[N=C](7) + φ[C–C=C]$(6)	708		697[b]	φ[C–C=C]$(15) + φ[C–C–C]$(12) + ν[N=C](10) + φ[C–N=C](10) + ω[C–H](10) + φ[N=C–C](9) + ω[C–N](8) +
657	–	–	φ[C–N=C](30) + ω[C–N](22) + ω[N=C](14) + φ[C–C=C]*(5) + τ[C=C]$(5) + τ[C–C]*(5)	629	–	–	φ[N=C–C](61) + τ[C–N](7) + ν[C–C]$(7) + τ[N=C](6) + φ[C–C–N](6) + φ[C=C–N](6)
649	–	–	φ[N=C–C](51) + φ[C=C–N](12) + φ[C–C–N](12) + τ[C–N](7) + ν[C–C]$(6) + τ[N=C](6)	618	–	–	ω[C–N](24) + φ[C–N=C](18) + φ[C–C=C]*(13) + ω[C–H](8) + τ[C–C]*(7) + τ[C–C]*(6)
614	–	624[c]	φ[C–C=C]*(69) + φ[H–C–C]*(11) + φ[H–C=C]*(7)	617	–	624[c]	φ[C–C=C]*(66) + φ[H–C–C]*(10) + φ[H–C=C]*(6) + ν[C=C]*(6) +
544	–	–	φ[N=C–C](35) + φ[C–C–N](11) + φ[C=C–N](10) + τ[C–N](10) + τ[N=C](10) + ν[C–C]$(9) + ν[C=C]$(6)	593	–	–	φ[C–N=C](19) + ω[N=C](17) + ω[C–N](11) + ω[C–H](9) + τ[C=C]$(9) + φ[C–C–C]$(7) + φ[N=C–C](5)
543	–	542[b]	ω[C–N](28) + ω[N=C](27) + τ[C=C]$(12) + τ[C–C]*(9) + τ[C=C]*(8)	577	–	–	φ[N=C–C](25) + φ[C=C–N](18) + φ[C–C–N](18) + τ[N=C](9) + τ[C–N](9) + ν[C–C]$(7) + φ[C–C=C]*(6)
519	518[b]	–	φ[C–C=C]$(66) + φ[H–C=C]$(14) + φ[C–C–H]$(9) + 6) ν[C–C]$(9)	519	518[b]	–	φ[C–C=C]$(66) + φ[H–C=C]$(14) + φ[C–C–H]$(9) + ν[C–C]$(9)
498		498[b]	ω[C–n](36) + ν[C–N](9) + ν[N=C](8) + ω[C–H](7) + φ[C–N=C](6.52)	505		498[b]	ω[N=C](24) + ω[C–N](23) + τ[C–C]*(12) + τ[C=C]*(11) + φ[C–N=C](8) + φ[C–C=C]*(7) + ω[C–H](6)
482	–	498[b]	φ[C–C=C]*(27) + φ[C–C–C]$(14) + φ[N=C–C](11) + φ[C–C=C]$(7) + ν[C–N](6) + τ[C=C]$(5)	498	–	498[b]	ω[C–N](35) + ω[N=C](27) + τ[C=C]$(18) + ω[C–H](7) + τ[C–C]$(7)

(*Continues*)

Table 2.
(Continued)

Cal. freq.	Obs. Freq.		Assignment (% PED), $\delta = 0$	Cal. freq	Obs. Freq.		Assignment (% PED), $\delta = \pi$
	Raman	IR			Raman	IR	
442	438[b]	–	ω[N=C](53) + ω[C–N](24) + ω[C–H](7) + τ[C–C]$(5)	379	374[b]	–	ω[C–N](20) + φ[C–C–C]$(17) + φ[N=C–C](13) + φ[C–C=C]$(8) + τ[C–C]$(7) + φ[C–N=C](6) + ν[N=C](5)
406	–	410[b]	τ[C–C]$(14) + φ[C–N=C](13) + τ[C=C]$ (12) + τ[C–C]*(11) + τ[C=C]*(10) + φ[C–C–C]$(7) + φ[N=C–C](6)	374	374[b]	–	ω[N=C](37) + φ[C–C=C]*(22) + ν[C–N](12) + τ[C–C]$(10)
358	359[b]	–	φ[C=C–N](31) + φ[C–C–N](31) + φ[N=C–C](29)	286		–	φ[N=C–C](31) + φ[C=C–N](24) + φ[C–C–N](24)
284	–	–	τ[C=C]$(55) + τ[C–C]$(24) + ω[C–H](17)	283		–	τ[C=C]$(52) + τ[C–C]$(22) + ω[C–H](15)
272	–	–	τ[C–C]*(42) + τ[C=C]*(38) + ω[C–H](15)	275		–	τ[C–C]*(33) + τ[C=C]*(29) + ω[C–H](11) + φ[N=C–C](7) + τ[C–N](6)
224		–	τ[C–C]$(27) + τ[C–C]*(16) + τ[C=C]*(15) + ω[N=C](13) + ω[C–N](11) + ω[C–H](11)	264		–	τ[C–C]$(37) + φ[C–N=C](11) + τ[C=C]$ (8) + ω[C–H](8) + ω[N=C](7) + φ[C–C–C]$(6)
202	–	–	τ[C–C]$(11) + τ[C–C]*(10) + φ[C–C=C]*(9.52) + τ[C=C]*(9) + ν[C–N](8) + φ[C–C–C]$(8) + φ[N=C–C](6) + ν[N=C](6) + ω[C–H](5)	263		–	φ[C–C–N](23) + φ[C=C–N](21) + φ[N=C–C](17) + τ[C–C]*(11) + τ[C=C]*(8) + τ[N=C](8)
200	212[b]	–	φ[C–N=C](42) + τ[C–C]$(16) + ω[N=C](15) + ω[C–N](7) + τ[C–C]*(7) + τ[C=C]*(7)	259		–	τ[C–C]*(26) + τ[C=C]*(26) + φ[C–N=C](10) + ω[C–H](8) + ω[C–N](6) + ω[N=C](6) + φ[C–C=C]*(5)
190	–	–	φ[N=C–C](31) + φ[C=C–N](27) + φ[C–C–N](26)	116	–	–	φ[C–N=C](30) + τ[C–C]$(26) + ω[C–N](16) + τ[C–C]*(6) + τ[C=C]*(6)
91	–	–	τ [C–N](46) + τ [N=C](35) + φ[N=C–C](7)	111	–	–	φ[C–N=C](28) + ω[N=C](20) + τ[C–C]*(13) + τ[C=C]*(12) + τ[C–C]$(12)
66	–	–	τ[C–C]$(41) + τ[C–C]*(22) + τ[C=C]*(21) + ω[C–H](12)	64	–	–	τ[C–N](87) + φ[N=C–C](10)
65	–	–	τ[N=C](55) + τ[C–N](44)	60	–	–	τ [C–N](83)

Note: 1. [a]Ref.-[30], [b]Ref.[29], [c]Ref.-[45]; 2. All freq. are in cm^{-1}; 3. ν, φ, ω and τ denote stretch, angle bend, wag and torsion respectively; 4 * and $ stands for benzoid and quinoid ring respectively.

1324 and 1317 cm^{-1}. The mode calculated at 1327 cm^{-1} is associated with the C–H bending mode of benzene ring, at 1324 cm^{-1} is associated with C–H bending mode of the quinoid ring and the mode at 1317 cm^{-1} is a mix C–H bending mode of benzoid and quinoid ring.

Mode calculated at 1176 cm^{-1} is associated with C–H bending mode of benzoid ring and normal mode calculated with 1154 cm^{-1} is with quinoid ring and these modes corresponds to the Wilson vibration 9a of p-disubstituted benzenes which are assigned to Raman peaks at 1164 and 1157 cm^{-1} respectively. The 18b vibration appears at 1098 cm^{-1} in the IR spectra and is assigned to the calculated normal mode at 1087 cm^{-1}. The mode calculated at 1008 cm^{-1} is a mixed mode of CCC bend and C–H bending of the benzene ring and is assigned to the IR weak band at 1006 cm^{-1}, can be seen as 18a Wilson vibrational mode.

C–N Stretching Vibrations

In the Raman as well as in IR spectra the most intense band is at 1480 cm^{-1}, this band is not seen in the reduced form of PANI and its oligomers and hence we can conclude that this band should be characteristic of oxidized form. Consequently, this band is assigned to C=N stretching mode. In the p-disubstituted benzenes the C–X (X=N in the PANI) stretching vibrational mode are no. 13 and 7a. In the spectra of PANI PNB

form we have a band at about 1211 (IR) and 1215 cm^{-1} (Raman) that can be assigned to the calculated modes at 1217 and 1214 cm^{-1} respectively that have N=C & N–C stretching vibrations as the main contribution in their PED.

C–H Out-of-Plane Vibrations

In the p-disubstituted benzenes normal vibration 17a, 10a, 10b and 11 are classified as C–H out of plane vibrations. The IR dip at 965 cm^{-1} is assigned to the calculated modes at 978 & 966 cm^{-1} and can be seen as 17a vibration of the quinoid and benzoid ring respectively. In the IR spectra we have a dip around 950 and 931 cm^{-1} and these dips can be seen as 10b vibration of the quinoid and benzoid rings and are assigned to the calculated modes at 948 and 938 cm^{-1}. Bands at 845(IR), 790 cm^{-1} (Raman) are found to be associated with 10a vibration of the benzoid and quinoid ring respectively and the IR bands at 775 and 750 cm^{-1} are with Wilson vibration no. 11.

Radial Skeletal Vibrations

Radial skeletal vibrations of the p-disubstituted benzenes are the Wilson no. 1, 12, 6a & 6b. Wilson no. 1 and 12 both vibrations are C–N stretch sensitive and appear in mix. After examining the PED of the modes calculated at 776 (assigned to the IR band at 775 cm^{-1}) & 708 cm^{-1} are completely mixed modes having radial skeletal vibrations of the benzoid and quinoid rings and can be seen as vibration 1 & vibration 12. The mode calculated at 614 and 519 cm^{-1} (assigned to the bands at 624(IR) and 518(Raman) cm^{-1} respectively) are associated with the radial skeletal vibrations of the benzoid (Wilson no. 6b) and quinoid ring (Wilson no. 6a) respectively.

Out-of-Plane Skeletal Vibrations

Wilson no. 4, 16a & 16b corresponds to the out-of-plane skeletal vibrations in p-disubstituted benzenes. Normal mode calculated at 718 cm^{-1} has C–C=C out-of-plane bend of the benzene ring and C–N stretch vibrations as the major component in the PED and can be seen as Wilson vibration 4. In PANI PNB form, IR dip at 498 cm^{-1} is assigned to the calculated mode at 498 and 482 cm^{-1}. Calculated normal mode at 498 cm^{-1} is purely associated with the out-of-plane skeletal vibrations of the quinoid ring (Wilson no.16b) and the mode calculated at 482 cm^{-1} is associated with out-of-plane skeletal vibrations of both benzoid and quinoid rings (Wilson no.16b). The band at 410 cm^{-1} is assigned to the calculated normal mode at 406 cm^{-1} and corresponds to 16a Wilson no. and is associated mainly with out-of-plane skeletal vibrations of the quinoid and benzoid rings.

C–N in-Plane Bending Vibrations

In p-disubstituted benzenes C–X (for PANI X=N) in-plane bending normal vibrations are 9b and 15. The Raman peak at 359 cm^{-1} is assigned to the calculated normal mode at 358 cm^{-1} and is associated with C–N in-plane bending vibrations and can be seen as 9b Wilson vibration. Calculated normal mode at 190 cm^{-1} is also C–N in-plane bending vibration and is assigned as Wilson vibration 15.

C–N Out-of-Plane Vibrations

Raman peak at 374 cm^{-1} is assigned to the calculated mode at zone boundary at 379 and 374 cm^{-1}, these modes are associated with out-of-plane C–N bend and can be seen as Wilson no. 5 vibration. Raman peak at 212 cm^{-1} is assigned to the modes calculated at 224, 202 & 200 cm^{-1}. These modes are associated with out-of-plane C–N vibrations and can be seen as 17b in-phase out-of-plane C–N vibration.

Dispersion Curves

In general, the IR absorption spectra and Raman spectra from polymeric systems are complex and can not be unravelled without the full knowledge of the dispersion curves. Besides providing knowledge of density-of-states, dispersion curves give information on the extent to the coupling of a mode along the chain in the ordered state. Dispersion curves and frequency distribution function are important for an understanding of thermodynamical and elastic

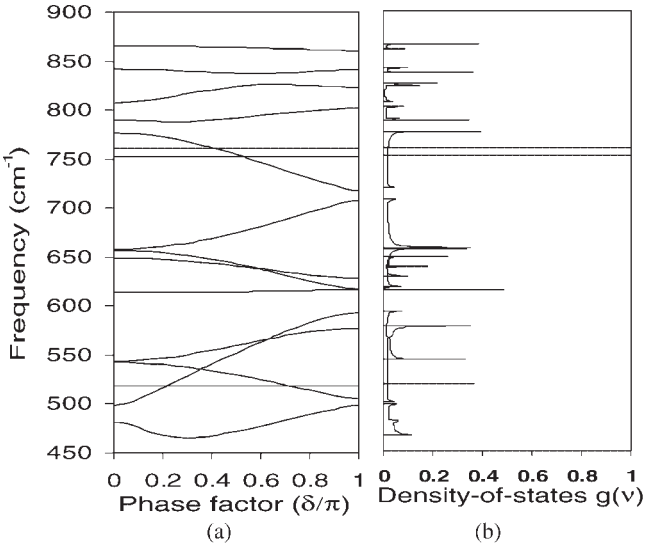

Figure 2.
(a) Dispersion curves and (b) Density of states of PANI PNB form (900–450 cm^{-1}).

properties of solids. Also a study of these is necessary to appreciate the origin of both symmetry independent and symmetry dependent spectral features. The dispersion curves of pernigraniline are shown in Figure 2(a) for frequencies 450–900 cm^{-1} and in Figure 3(a) 0–450 cm^{-1} for frequencies. The dispersion curves above 900 cm^{-1} are not shown because they have negligible dispersion.

The modes of PANI PNB have some special features like crossing. All such modes showing crossover are listed in Table 3 along with the PED and the δ values at which these features occur. To ascertain whether it is a crossing or a repulsion calcu-

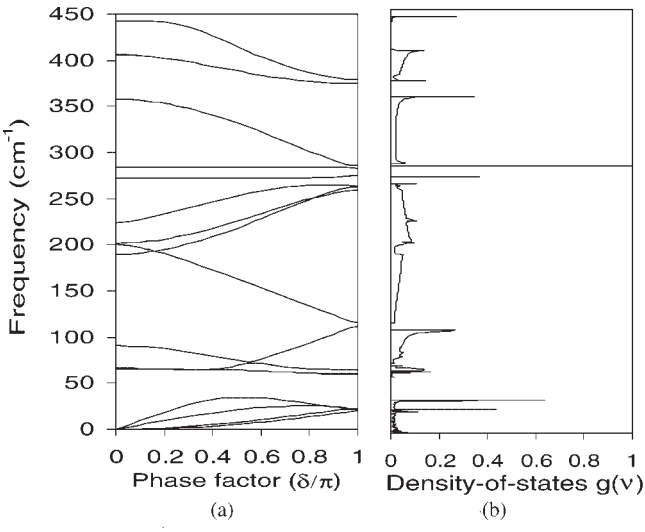

Figure 3.
(a) Dispersion curves and (b) Density of states of PANI PNB from 0–450 cm^{-1}.

Table 3.
Crossing between the pair of modes of PANI PNB form

Freq.($\delta = 0$)	Before Crossing				After Crossing		
	$\delta^{\#}/\Pi$	δ^{*}/Π	Freq.	PED	δ^{*}/Π	Freq.	PED
i							
776	0.419	0.40	762	ν[C–C]$ (15) + ν[C–N] (12) + φ[C–C=C]*(11) + φ[C–C=C]$(10) + φ[C–C–C]$ (8) + φ[C–N=C] (6) + φ[N=C–C] (6) + ν[N=C] (6)	0.45	761	ω[C–H] (84) + τ[C–C]* (7) + τ[C=C]*(7)
761	0.419	0.40	761	ω[C–H] (83) + τ[C=C]*(7) + τ[C–C]*(7)	0.45	758	ν[C–C]$(15) + ν[C–N] (12) + φ[C–C=C]*(11) + φ[C–C=C]$(10) + φ[C–C–C]$(8) + φ[C–N=C] (7)
ii							
761	0.532	0.50	755	ν[C–C]$ (15) + ν[C–N](12) + a[C–C=C]* (11) + a[C–C=C]$(9) + a[C–C–C]$(8) + a[C–N=C](7) + ν[N=C] (6) + a[N=C–C](6)	0.55	752	ω[C–H](86) + τ[C–C]$(14)
752	0.532	0.50	752	ω[C–H] (86) + τ[C–C]$ (14)	0.55	751	ν[C–C]$(14) + ν[C–N]*(12) + a[C–C=C]*(11) + a[C–C=C]$(9) + a[C–N=C](8) + a[C–C–C]$(8) + ν[N=C](6) + a[N=C–C] (6)
iii							
657	0.589	0.55	641	φ[C–N=C](24) + ω[C–N] (20) + ω[N=C](11) + φ[C–C=C]*(7) + ω[C–H] (6)	0.65	636	φ[N=C–C] (54) + φ[C–C–N](9) + φ[C=C–N] (8) + τ[C–N] (7) + ν[C–C]$(6) + τ[N=C](6)
649	0.589	0.55	640	φ[N=C–C] (52) + φ[C=C–N](10) + φ[C–C–N](9) + τ[C–N](6) + ν[C–C]$(6) + τ[N=C] (6)	0.65	635	φ[C–N=C] (23) + ω[C–N](21) + ω[N=C](11) + φ[C–C=C]* (8) + ω[C–H] (7)
iv							
544	0.629	0.60	565	φ[N=C–C] (30) + φ[C–C–N](16) + φ[C=C–N] (15) + τ[N=C](9) + τ[C–N](9) + ν[C–C]$(8) + ν[C=C]$(5)	0.65	569	ω[C–N](14) + φ[C–N=C](13) + ω[N=C](11) + φ[C–C=C]*(8) + ω[C–H] (8) + φ[C–C–C]$(7) + φ[N=C–C](6) + ν[C–N] (5)
543	0.629	0.60	563	ω[C–N](15) + φ[C–N=C] (12) + ω[N=C](10) + φ[C–C=C]*(9) + ω[C–H] (8) + φ[C–C–C]$(7) + φ[N=C–C](6) + ν[C–N](5)	0.65	567	φ[N=C–C] (29) + φ[C=C–N] (16) + φ[C–C–N] (15) + τ[N=C] (9) + τ[C–N](9) + ν[C–C]$(8) + ν[C=C]$ (5)
v							
543	0.357	0.35	536	ω[C–N] (27) + ω[N=C] (26) + τ[C=C]$(11) + τ[C–C]*(9) + τ[C=C]*(8)	0.40	541	ω[C–N] (16) + φ[C–C=C]* (11) + φ[C–N=C] (9) + ω[N=C] (8) + φ[C–C–C]$ (8) + ω[C–H] (6) + ν[C–N](6) + φ[N=C–C] (6)
519	0.357	0.35	535	ω[C–N] (17) + φ[C–C=C]*(10) + φ[C–N=C] (9) + ω[N=C] (8) + φ[C–C–C]$(8) + ν[C–N] (7) + ω[C–H] (6) + φ[N=C–C] (6)	0.40	534	ω[C–N] (27) + ω[N=C] (26) + τ[C=C]$ (11) + τ[C–C]*(9) + τ[C=C]* (8)
vi							
519	0.713	0.70	520	ω[C–N] (27) + ω[N=C] (26) + τ[C=C]$ (9) + τ[C–C]*(9) + τ[C=C]* (8)	0.75	519	φ[C–C=C]$ (66) + φ[H–C=C]$ (14) + φ[C–C–H]$ (9) + ν[C–C]$(9)
498	0.713	0.70	519	φ[C–C=C]$(66) + φ[H–C=C]$ (14) + φ[C–C–H]$ (9) + ν[C–C]$ (9)	0.75	519	ω[C–N] (27) + ω[N=C] (26) + τ[C–C]* (9) + τ[C=C]$ (8) + τ[C=C]* (8)
vii							
519	0.219	0.20	519	φ[C–C=C]$ (66) + φ[H–C=C]$(14) + φ[C–C–H]$(9) + ν[C–C]$(9)	0.25	523	ω[C–N](19) + φ[C–C=C]*(11) + φ[C–C–C]$(7) + φ[C–N=C] (7) + ν[C–N](7) + ω[N=C](7) + φ[N=C–C](6) + ω[C–H](6)
498	0.219	0.20	517	ω[C–N](20) + φ[C–C=C]*(10) + ν[C–N] (7) + φ[C–C–C]$ (7) + φ[C–N=C](7) + ω[N=C] (6) + φ[N=C–C] (6) + ω[C–H] (6)	0.25	519	φ[C–C=C]$ (66) + φ[H–C=C]$ (14) + φ[C–C–H]$(9) + ν[C–C]$ (9)
viii							
202	.826	0.80	250	τ[C–C]*(15) + τ[C=C]*(14) + τ[C–C]$ (11) + ω[C–H] (7) + φ[C–N=C](7) + φ[C–C=C]* (6)	0.85	254	φ[C–C–N] (26) + φ[N=C–C] (24) + φ[C=C–N] (23) + τ[N=C] (7)

(*Continues*)

Table 3.
(Continued)

Freq.($\delta = 0$)	Before Crossing				After Crossing		
	$\delta^{\#}/\Pi$	δ^{*}/Π	Freq.	PED	δ^{*}/Π	Freq.	PED
200	.826	0.80	249	φ[C=C–N] (26) + φ[N=C–C] (25) + a[C–C–N] (23) + τ[N=C](7)	0.85	253	τ[C–C]*(16) + τ[C=C]* (16) + τ[C–C]$ (10) + a[C–N=C] (8) + ω[C–H] (7) + a[C–C=C]* (5)
ix							
200	0.163	0.15	194	φ[C–N=C] (36) + τ[C–C]$ (18) + ω[N=C](15) + τ[C–C]*(9) + ω[C–N](8) + τ[C=C]*(8)	0.20	195	φ[N=C–C] (31) + φ[C=C–N] (26) + φ[C–C–N] (26)
189	0.163	0.15	193	φ[N=C–C] (31) + φ[C=C–N] (26) + φ[C–C–N] (26)	0.20	190	φ[C–N=C] (34) + τ[C–C]$ (18) + ω[N=C] (14) + τ[C–C]*(9) + ω[C–N](8) + τ[C=C]*(8)
x							
91	0.559	0.55	73	τ[C–N] (56) + τ[N=C] (22) + φ[N=C–C] (9) + φ[C=C–N] (5)	0.60	76	τ[C–C]$ (24) + φ[C–N=C] (22) + τ[C–C]* (13) + τ[C=C]*(12) + ω[N=C] (8) + ω[C–H] (7) + ω[C–N] (6)
66	0.559	0.55	72	τ[C–C]$ (26) + φ[C–N=C] (18) + τ[C–C]* (14) + τ[C=C]* (13) + ω[C–H] (7) + ω[N=C] (7)	0.60	71	τ[C–N] (60) + τ[N=C] (18) + φ[N=C–C] (10)
xi							
66	0.348	0.30	65	τ[N=C] (54) + τ[C–N] (40)	0.40	65	τ[C–C]$(35) +) τ[C–C]*(19) + τ[C=C]* (18) + ω[C–H] (10) + φ[C–N=C] (7)
65	0.348	0.30	64	τ[C–C]$ (37) + τ[C–C]*(20) + τ[C=C]*(19) + ω[C–H] (11)	0.40	64	τ[N=C] (57) + τ[C–N] (39)
xii							
66	0.196	0.15	65	τ[C–C]$ (39) + τ[C–C]*(22) + τ[C=C]* (20) + ω[C–H] (11)	0.25	65	τ[N=C] (53) + τ[C–N] (41)
65	0.196	0.15	65	τ[N=C] (53) + τ[C–N] (42)	0.25	65	τ[C–C]$ (38) + τ[C–C]* (21) + τ[C=C]* (19) + ω[C–H] (11)
xiii							
0.00	0.966	0.95	22	τ[C–C]$ (23) + τ[C–C]*(18) + φ[C–N=C](17) + τ[C=C]* (17) + ω[C–H] (9) + ω[N=C](8) + ω[C–N] (8)	0.97	22	τ[N=C] (49) + τ[C–N](36)
0.00	0.966	0.95	21	τ[N=C] (47) + τ[C–N](38)	0.97	22	τ[C–C]* (20) + τ[C–C]$(19) + τ[C=C]*(18) + φ[C–N=C](17) + ω[C–H] (9) + ω[C–N] (8) + ω[N=C] (8) +
xiv							
0.00	0.883	0.85	26	τ[C–C]$ (26) + φ[C–N=C] (18) + τ[C–C]* (16) + τ[C=C]* (14) + ω[N=C] (9) + ω[C–H] (9) + ω[C–N] (8)	0.90	25	τ[C–N] (46) + τ[N=C] (43)
0.00	0.883	0.85	25	τ[C–C]$ (26) + φ[C–N=C] (18) + τ[C–C]* (16) + τ[C=C]* (14) + ω[N=C] (9) + ω[C–H] (9) + ω[C–N] (8)	0.90	25	τ[C–C]$ (25) + φ[C–N=C] (17) + τ[C–C]* (16) + τ[C=C]* (15) + ω[C–H] (9) + ω[N=C] (9) + ω[C–N] (8)

Note: 1. δ# corresponds to crossing points; 2. δ^{*} corresponds to the points before/after crossing.

lations at very close intervals of $\delta = .001\ \pi$ have been performed and it was found that the modes cross-over. From symmetry considerations, it can be shown that when the approaching modes belong to different symmetry species then they can crossover. Since PANI PNB form has mirror plane of symmetry along the chain axis, hence crossing are permissible.[46] Therefore, no two dispersion curves both of which belong to the same symmetry species can cross because this would imply the existence of two modes of vibrations with the same symmetry species and same frequency. This is also obvious from the Table 3 in which we have shown the pair of modes, which cross, belongs to different symmetries, i.e. in plane and out-of-plane modes. Such cross-over occurs in the case of pair of modes at 776 & 761 cm^{-1}, 776 & 752 cm^{-1}, 657 &

649 cm^{-1}, 544 and 498 cm^{-1}, 543 & 498 cm^{-1}, 543 & 519 cm^{-1}, 519 & 498 cm^{-1}, 202 & 189 cm^{-1}, 91 & 66 cm^{-1}, 66 & 65 cm^{-1} and acoustic modes which cross each other once or twice. The intersection phenomenon of modes can be regarded as an inelastic collision of two phonons in energy momentum space.

Study of dispersion curves enables the calculation of frequency distribution function. The frequency distribution function (density-of-states) shows how the energy is distributed among the various branches of the normal modes. Figure 2(b) and 3(b) show the plots of density-of-states versus frequency as obtained from the dispersion curves. The peaks of the frequency distribution curves correspond to regions of high density-of-states (Von Hove type singularities).

As our calculations have been made for an isolated molecular chain, the interpretation of IR \ Raman spectral and theoretical calculations are subjected to certain limitations. A complete interpretation of the spectra requires calculations of a three dimensional system where interactions play an important role. The only additional correction in this work is to check the force field through the deuterated or isotopically substituted species of pernigraniline.

Conclusion

In this paper, a detailed investigation of the vibrational properties of PANI PNB form has been performed. The vibrations have been assigned based on para-disubstituted benzene derivatives which provides a better understanding of the spectra. Normal modes and set of force constants for the PANI PNB form are being obtained by Urey – Bradley force field and several new assignments are being reported. All the characteristic features of the dispersion curves such as regions of high density-of-states, cross-over and repulsion have been well interpreted from the vibrational dynamics of PANI PNB form. Similar studies on the lecuromeldine and emeraldine salts are in progress with the aim of determining the modifications induced by primary and secondary doping.

[1] L. A. Ray, G. E. Asturias, D. L. Kershur, A. F. Richter, A. G. MacDiarmid, A. J. Epstein, *Synth. Met.* **1989**, *29*, E141.
[2] K. G. Neoh, E. T. Kang, S. H. Khor, K. L. Tan, *Polym. Degrad. Stab.* **1990**, *27*, 107.
[3] K. L. Tan, B. T. G. Tan, E. T. Kang, K. G. Neoh, *J. Chem. Phys.* **1991**, *94*, 5382.
[4] H. Letheby, *J. Chem. Soc. 1862*(15), 161.
[5] de Surville, M. Jozefowicz, L. T. Yu, J. Perichon, R. Buvet, *Electrochim. Acta* **1968**, *13*, 1451.
[6] A. F. Diaz, J. A. Logan, *J. Electroanal. Chem.* **1980**, *111*, 111.
[7] T. Kobayashi, H. Yoneyama, H. Tamura, *J. Electroanal. Chem.* **1984**, *177*, 281.
[8] E. M. Genies, C. Tsintavis, *J. Electroanal. Chem.* **1984**, *195*, 109.
[9] A. G. Macdiarmid, S. L. Mu, N. L. D. Somasiri, W. Wu, *Mol. Cryst. Lig. Cryst.* **1985**, *121*, 181.
[10] E. M. Genies, A. A. Syed, C. Tsintavis, *Mol. Cryst. Lig. Cryst.* **1985**, *121*, 187.
[11] W. R. Salaneck, I. Lundstrom, B. Liedberg, M. A. Hasan, R. Erlandsson, P. Konradsson, A. G. Macdiarmid, N. L. D. Somasiri, *Springer Ser. Solid State Sci.* **1985**, *63*, 218.
[12] L. W. Schacklette, M. Maxfield, S. Gould, J. F. Wolf, T. R. Jow, R. H. Baughman, *Synth. Met.* **1987**, *18*, 611.
[13] K. Okabayashi, F. Goto, K. Abe, T. Yoshida, *Synth. Met.* **1987**, *18*, 365.
[14] A. G. Macdiarmid, L. S. Yang, W. S. Haung, B. D. Humphrey, *Synth. Met.* **1987**, *18*, 611.
[15] E. M. Genies, P. Hany, Ch. Santier, *J. Appl. Electrochem.* **1988**, *18*, 751.
[16] W. Wang, G. Li, C. Li, F. Wang, *J. Appl. Electrochem.* **1988**, *18*, 751.
[17] E. W. Paul, A. J. Ricco, M. S. Wrighton, *J. Phys. Chem.* **1985**, *89*, 1441.
[18] A. Boyle, E. M. Genies, M. Lapkowski, *Proceedings of ICSM'88, Santa Fe/USA, Synth. Metals* **1989**, *63*, 211.
[19] T. Kobayashi, H. Yoneyama, H. Tamura, *J. Electroanal. Chem.* **1984**, *161*, 419.
[20] A. Kitani, J. Yano, K. Sasaki, *J. Electroanal. Chem.* **1986**, *209*, 227.
[21] B. Aurian-Blajeni, I. Taniguchi, J. O. M̀. Bochris, *J. Electroanal. Chem.* **1983**, 149, 291.
[22] A. G. Green, A. E. Woodhead, *J. Chem. Soc. Trans.* **1910**, *97*, 2388.
[23] A. G. Green, A. E. Woodhead, *J. Chem. Soc. Trans.* **1912**, *101*, 1117.
[24] A. Ray, A. F. Richter, A. G. Macdiarmid, A. J. Epstein, *Synth. Met.* **1989**, *29*, 151.
[25] A. Ray, G. E. Asturias, D. L. Kershner, A. F. Richter, A. G. Macdiarmid, A. J. Epstein, *Synth. Met.* **1989**, *29*, E141.; A. Ray, A. F. Richter, A. G. Macdiarmid, A. J. Epstein, *Synth. Met.* **1989**, *29*, E151.
[26] T. Shimanouchi, *J. Chem. Phys.* **1949**, *17*, 245.
[27] H. G. Urey, C. A. Bradley, *Phys. Rev.* **1931**, *38*, 1969.

[28] S. Quillard, G. Louarn, S. Lefrant, A. G. Macdiarmid, *Physical Riew B* **1994**, *50*, 17,12496.
[29] M. Cochet, G. Louarn, S. Quillard, M. I. Boyer, J. P. Buisson, S. Lefrant, *J. Raman Spectrosc.* **2000**, *31*, 1029.
[30] M. I. Boyer, S. Quillard, E. Rebourt, G. Louarn, J. P. Buisson, A. Monkman, S. Lefrant, *J. Phys. Chem. B* **1998**, *102*, 782.
[31] W. Qian, N. G. Mirikin, S. Krimm, *Chem. Phys Lett.* **1999**, *315*, 125.
[32] G. Varsanyi, *Vibrational spectra of Benzene Derivatives*, Academic Press, New York **1969**, Chapter 3.
[33] F. R. Dollish, W. G. Fateley, F. F. Bentley, *Characteristic Raman, Frequencies of Organic Compounds*, Wiley, New York **1974**.
[34] N. B. Colthup, L. H. Daly, S. E. Wiberley, *Introduction to Infrared and Raman Spectroscopy*, Acedemic Press, Boston **1990**, Chapter 8.
[35] A. Stojiljkovic, D. H. Whiffen, *Spectrochim. Acta* **1958**, *12*, 47.
[36] A. Stojiljkovic, D. H. Whiffen, *Spectrochim. Acta* **1958**, *12*, 57.
[37] C. Garrigou-Lagrange, J. M. Lebas, M. L. Josien, *Spectrochim. Acta* **1958**, *12*, 305.
[38] D. H. Whiffen, *Spectrochim. Acta* **1955**, *7*, 253.
[39] R. R. Randle, D. H. Whiffen, *Molecular Spectroscopy*, Institute of Petroleum, London **1955**, p 111.
[40] E. B. Wilson, Jr., *J Chem Phys* **1939**, *7*, 1047.
[41] E. B. Wilson, Jr., *J Chem Phys* **1941**, *9*, 76.
[42] P. W. Higgs, *Proc Roy Soc London A* **1953**, *220*, 472.
[43] B. Mannfors, K. Palmo, S. Krimm, *J. Mol. Struct.* **2000**, *556*, 1.
[44] W. T. King, I. M. Mills, B. L. Crawford, *J. Chem. Phys.* **1957**, *27*, 455.
[45] H. Neugebauer, A. Neckel, N. S. Sariciftci, H. Kuzmany, *Synth. Metals* **1989**, *29*, E185.
[46] D. I. Bower, W. F. Maddams, *The vibrational spectroscopy of polymers*, Cambridge University Press, Cambridge **1989**.

